^{119}Sn Mössbauer Spectroscopy for assessing the local stress and defect state towards the tuning of Ni-Mn-Sn alloys

I. Unzueta,[1,2,a] J. López-García,[3,4] V. Sánchez-Alarcos,[4,5] V. Recarte,[4,5] J. I. Pérez-Landazábal,[4,5] J. A. Rodríguez-Velamazán,[3] J. S. Garitaonandia,[6,2] J. A. García,[6,2] and F. Plazaola[1]

[1)] *Department of Electricity and Electronics, University of the Basque Country UPV/EHU, 48940 Leioa, Spain*

[2)] *BCMaterials, University of Basque Country UPV/EHU, 48940 Leioa, Spain*

[3)] *Institut Laue-Langevin, 71 Avenue des Martyrs, 38000 Grenoble, France*

[4)] *Department of Physics, Universidad Pública de Navarra, Campus de Arrosadia, 31006 Pamplona, Spain*

[5)] *Institute for Advanced Materials (INAMAT), Universidad Pública de Navarra, Campus de Arrosadía, 31006 Pamplona, Spain*

[6)] *Department of Applied Physics II, University of the Basque Country UPV/EHU, 48940 Leioa, Spain*

The influence of defects and local stresses on the magnetic properties and martensitic transformation in $Ni_{50}Mn_{35}Sn_{15}$ is studied at macroscopic and atomic scale level. We show that both structural and magnetic properties of the alloy are very sensitive to slight microstructural distortions. Even though no atomic disorder is induced by milling, the antiphase boundaries linked to dislocations promote the antiferromagnetic coupling of Mn, resulting in a significant decrease in the saturation magnetization. On the other hand, the temperature range of the transformation is considerably affected by the mechanically-induced local stresses, which in turn does not affect the equilibrium temperature between the austenitic and martensitic phase. Finally, we demonstrate that the recovery of the martensitic transformation is directly related with the intensity of the non-magnetic component revealed by ^{119}Sn Mössbauer spectroscopy. This result opens the possibility of quantifying the whole contribution of defects and the local stresses on the martensitic transformation in Ni-Mn-Sn alloys.

Ni-Mn based Heusler alloys have been extensively studied during the last two decades due to the multifunctional properties they exhibit such as large magnetic-field-induced strain[1,2], magnetorresitivity[3,4], magnetocaloric effect[5–8], exchange bias[9,10] and shape-memory effect[11]. These properties are linked to the occurrence of a martensitic transformation (MT) between magnetically ordered phases. In the case of metamagnetic shape memory alloys, Ni_2Mn-Z (Z = In, Sn, Sb) the MT occurs between ferromagnetic austenite and weak magnetic martensite, thus giving rise to interesting properties such as magnetic-field induced shape memory effect[12–15] and inverse magnetocaloric effect[16–18].

Despite the promising features, these alloys present very poor mechanical properties and their brittleness and fragility hinder the development of practical devices. In order to overcome the limitations of the bulk material, several alternatives have been investigated, such as the use of alloys in form of ribbons[19], foams[20] or films[21], as well as embedding shape memory particles in a polymer matrix[22,23]. As a result, the use of microparticles as microactuator elements is attracting an increasing interest during the last years[24–27].

In order to enhance the multifunctional properties of the micro-particles and films, the control of defects and the local stress-state becomes fundamental as they influence directly the MT[28–31]. The presence of residual stress increases the thermal hysteresis and the irreversibility of the MT[32]. Residual stress is also retained when the samples are cycled through the phase transformation[33], being one of the main causes of the degradation of the MT, the deformation behavior, and the shape memory effect[34]. Additionally, the presence of defects induced during the synthesis of nanoparticles may inhibit the MT[35] and influence the ferromagnetic (FM) interactions as well[36]. Thus, the characterization of defects, the local stress-state and their influence on the MT will provide a more proper tuning of the structural and magnetic properties of these alloys for more extensive applications[27,37]. In particular, Ni-Mn-Sn alloys have been extensively studied because of their enhanced magnetocaloric properties[38] and the high stability of their long-range atomic order structure against thermal treatments[39].

[a)] Electronic mail: iraultza.unzueta@ehu.eus

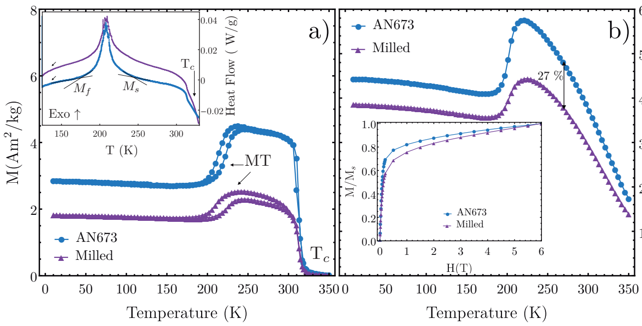

FIG. 1. (Color online) $M(T)$ for the Milled and AN673 sample recorded at 0.01 T (a) and 6 T (b). Inset in (a) shows the DSC of both samples. The inset in (b) shows the normalized $M(H)$ cycle of both Milled and AN673 sample recorded at 270 K.

Mössbauer spectroscopy (MS) is a powerful technique for both structural and magnetic characterization at atomic level. Although several works can be found in which ^{57}Fe MS has been used in Fe doped Ni-Mn-Sn alloys[36,40–42], ^{119}Sn MS, which makes doping unnecessary and therefore helps to ensure chemical environment of Sn atoms, has been scarcely employed[43]. In fact, the present work demonstrates that even though no atomic disorder is induced, defects and local stresses affect greatly the MT, which can be directly quantified by ^{119}Sn MS. The obtained results are especially interesting as long as the modification of defects configuration could be, along with composition, the only way to properly tune the functional properties in these systems.

A polycrystalline ingot of $Ni_{50}Mn_{35}Sn_{15}$ was synthesized from high purity elements by arc melting under protective argon atmosphere. The obtained alloy was homogenized at 1173 K during 24 h and its composition was checked by EDX analysis. With the aim of inducing defects, the alloy was mechanically milled in an agate mortar until reaching a steady state in the spectra revealed by ^{119}Sn MS. Then, in order to analyze the microstructural evolution upon post-milling, several milled powder samples were taken and separately annealed at 573, 673, 773 and 873 K during 5 minutes at each temperature (labeled as Milled, AN573, AN673, AN773 and AN873 respectively). Calorimetric measurements were carried out in a TA Q100 DSC at heating/cooling rate of 10 K/min and the magnetic characterization was performed using a QD MPMS XL-7 SQUID magnetometer. Powder neutron diffraction (PND) measurements were done at D2B instrument ($\lambda = 1.59$ Å) at the Institute Laue-Langevin in Grenoble (France)[44]. The FullProf[45] program was employed for the Rietveld refinement. Mössbauer spectra were obtained using a Ba^{119}SnO$_3$ source in a transmission setup at 270 K and fitted using NORMOS program.

Fig. 1 shows the temperature dependence of magnetization at 0.01 T (1(a)) and 6 T (1(b)) for both the Milled and the AN673 samples. As shown in Fig. 1(a), annealing does not affect neither the T_c nor the MT temperature (the same behaviour is observed for the rest of the AN573, AN773 and AN873 samples, not shown here). This can be also inferred from the DSC measurements (see inset of Fig. 1(a)), which, in turn, show a narrower temperature range of the MT for the AN673 sample, indicating a decrease in the elastic energy term as a result of annealing[29]. Taking into account that both T_c and the MT temperature are highly sensitive to atomic order[46], the lack of variation in these transition temperatures seems to indicate a null effect of annealing in the atomic order[39]. Nevertheless, as shown in Fig. 1(b), the high-field magnetization increases in both austenite and martensite on annealing. Furthermore, the different approach to saturation shown in the normalized $M(H)$ curves measured at 270 K (inset Fig. 1(b)) points out a different antiferromagnetic (AF) contribution to the magnetic moment between the Milled and AN673 samples.

The crystallographic structure and long-range atomic order of the studied samples have been analyzed from PND measurements. Fig. 2(a), 2(b) show the experimental and fitted diffractograms obtained on the Milled and AN673 samples at 270 K (ferromagnetic austenite). Both samples show the cubic L2_1 (Fm$\bar{3}$m) structure with the same lattice parameter (6.004(1) Å for the Milled sample and 6.003(1) Å for the AN673 sample). The magnetic and structural parameters for 4(a) and 4(b) positions obtained after Rietveld refinement are shown in Table I. The occupancies are almost the same in both cases (4(a) positions are mainly occupied by Mn atoms and 4b positions are occupied by both Mn and Sn atoms[47], as illustrated in Fig. 2(c)), which means that the degree of L2_1 atomic order is the same in both samples.Therefore, in agreement with the observed absence of variation in the transition temperatures, no atomic order variation is brought by annealing. Nevertheless, interestingly, the magnetic coupling between Mn atoms in 4a and 4b positions drastically evolves from AF to FM upon annealing, in spite of neither atomic order nor lattice parameter does. Such evolution is indeed in line with the observed increase in the high-field magnetization. In this respect, it is worth noting that the reflection peaks are clearly broader in the Milled sample. This points out a microstructural evolution (higher crystallite size or lower microstrains in the annealed sample), which could be behind the magnetic one.

In order to ascertain the nature of the effect of annealing on the magnetic properties, the magnetism has been studied at atomic level by ^{119}Sn MS. Fig. 3 shows the experimental and fitted ^{119}Sn Mössbauer spectra for all the samples. The spectrum of the Milled sample is mainly composed by a non-magnetic singlet with a non-resolved magnetic component as a minor contribution. The relative intensity of both components changes gradually with the annealing temperature, being the magnetic subspectrum practically the only contribution to the spectrum of the AN873 sample. All the spectra have been satisfactorily fitted exclusively with these two discrete contribu-

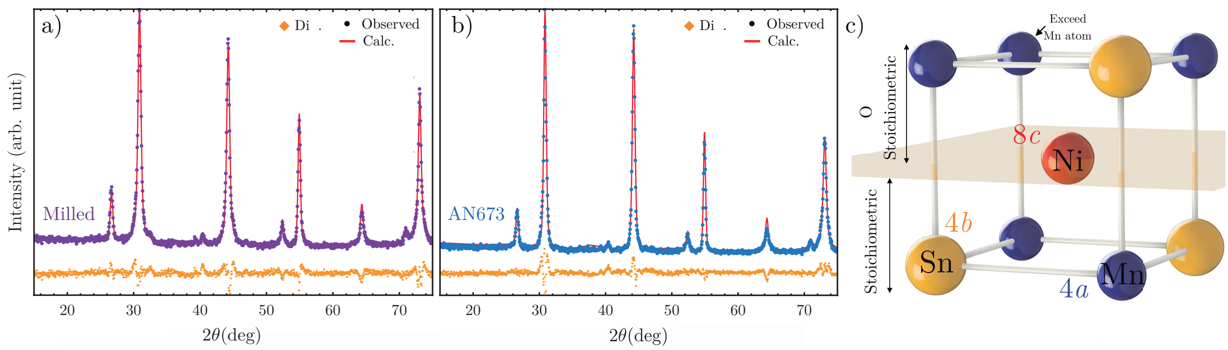

FIG. 2. (Color online) Rietveld refinement of the diffraction patterns for the Milled (a) and AN673 samples (b) recorded at 270 K. (*c*) Preferred positions of Mn and Sn atoms in stoichiometric and off-stoichiometric samples.

tions.

The values obtained from the fitting of Mössbauer spectra are listed in Table II. The main common feature is the decrease of the singlet component (A_s) and the B_{hf} magnetic hyperfine field increase, with increasing the annealing temperature. Similar values of the δ isomer shift of both components have been obtained for all the samples, indicating that the chemical order in the surrounding of Sn atoms remains the same independently of the annealing process[48]. However, the line-width parameter Γ listed in Table II decreases as the annealing temperature increases. The Γ parameter is sensitive to the slight distortions of the local environment of the Mössbauer probe atoms[49] so its decrease indicates a microstructural recovery on the very close environment of Sn atoms.

In a nutshell, PND, MS and magnetic measurements point out the lack of atomic disorder differences between the studied samples. However, the decrease of Γ parameter and the narrowing of the PND peaks with the annealing temperature increase, suggest a evolution in the microstructural parameters. Thereby, the observed changes on the magnetic properties and in the width of the MT would rely on different internal stress state and the presence of defects created during the milling.

As previously reported in some Heusler alloys, several local distortions as dislocations and defects can be created during mechanical treatments (i. e. cold working) without inducing any atomic disorder[50,51]. Specifically, the presence of superlattice dislocations in cold worked Heusler alloys are accompanied by anti-phase boundaries (APB)[52,53]. Besides, the exchange interaction between the second nearest neighbor (SNN) Mn atoms located across the APB can become AF in an otherwise FM material[54,55].

Although the SNN of Mn are Sn atoms at 4*b* positions, in off-stoichiometric conditions the excess Mn occupy 4*b* positions (see Fig. 2(c)). As listed in Table I, the coupling of 4*a* and 4*b* positions is mostly AF in the Milled sample. However, when the samples are annealed, the FM coupling is recovered. Taking into account that the

	Site 4*a*		Site 4*b*		Site 8*c*
	Occupancy	$\mu(\mu_B)$	Occupancy	$\mu(\mu_B)$	Occupancy
Milled	Mn 0.95(4) Ni 0.05(4) Sn (—)	1.26(6)	Mn 0.41(4) Ni 0.02(0) Sn 0.57(4)	-0.45(6)	Mn 0.08(1) Ni 0.92(1) Sn (—)
AN673	Mn 0.94(3) Ni 0.06(3) Sn (—)	2.58(2)	Mn 0.43(3) Ni 0.05(0) Sn 0.52(3)	0.37(2)	Mn (—) Ni 1(-) Sn (—)

Table I. Occupancies and magnetic moment values (μ) for 4*a*, 4*b* and 8*c* positions obtained from the Rietveld refinement for the Milled and AN673 samples. For 8*c* position $\mu = 0$ is considered.

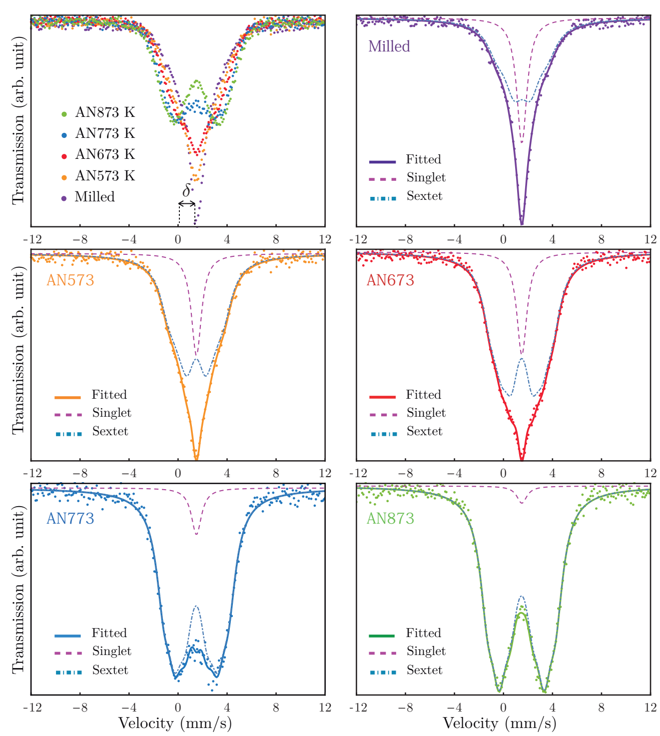

FIG. 3. (Color online) Raw (up left) and fitted Mössbauer spectra for the Milled and all annealed samples at 270 K.

Sample	$\delta(mm/s)$[a]	$\Gamma(mm/s)$[a]	B_{hf} (T)	A_s (%)
Milled	1.53(1)	1.96(1)	4.1(1)	%31(3)
AN573	1.48(1)	1.67(7)	4.6(2)	%18(1)
AN673	1.48(1)	1.54(5)	5.2(1)	%15(1)
AN773	1.48(1)	1.51(4)	5.3(1)	%6(1)
AN873	1.48(1)	1.50(2)	5.6(1)	%1(1)

[a] Constrained to be the same for both subspectra.

Table II. δ isomer shift, Γ line-width, the hyperfine field B_{hf} and the area of the singlet component A_s obtained from the fitting procedure of the Mössbauer spectra for all the studied samples.

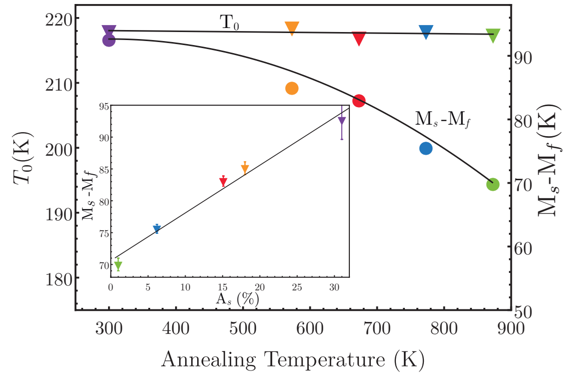

FIG. 4. (Color online) Evolution of the T_0 parameter (triangles) and the M_s-M_f (full dots) as a function of the annealing temperature. The inset shows the mutual dependence between the M_s-M_f parameter and A_s.

number of AF coupled Mn atoms is proportional to the dislocation density[52], the annihilation of dislocations results on a decrease of the density of the APB present in the sample, in such a way that the number of AF coupled Mn atoms decreases and the FM coupling is reinforced. Hence, the magnetization is greater in the AN673 sample than in the Milled sample. Additionally, as shown in Fig. 1(b) the magnetization of the AN673 sample approaches better the saturation than the Milled sample.

The annihilation of dislocations also explains the reduction of Γ parameter and the narrowing of PND peaks after the annealing[55]. The release of the local stress associated to dislocations homogenizes the surrounding environment of Sn atoms and, as a consequence, the value of Γ decreases. As shown in Table II, the major recovery of Γ occurs in the first two annealing at 573 K and 673 K. The annihilation of the dislocations at these temperatures has been previously reported in other Heusler alloys[50,53]. However, as the ^{119}Sn MS shows in Fig. 3, the recovery process continues above 673 K without a significant change on Γ. In this region, the recovery would be mediated by the elimination of point defects such as vacancies[56].

Sn atoms do not carry intrinsic magnetic moment, but a transferred hyperfine field can be induced from the neighboring magnetic ions (Mn ions in the case of Ni-Mn-Sn)[57]. ^{119}Sn Mössbauer spectra would reflect the local magnetic field felt by the Sn atoms. The singlet component observed by MS (Fig. 3), related to stressed regions caused by dislocations and APB, indicates absence of local magnetic field. Thus, this component points out that the ferromagnetic order is altered in the region of influence of the APB in such a way that the total transferred dipolar field at Sn sites is zero. A_s decreases as soon as the density of dislocations and APB decreases with annealing at higher temperatures. On the contrary, the B_{hf} at 4b positions increases (see Table I). In fact, B_{hf} is $\approx$ 27% higher in AN673 than in the Milled sample, that is exactly the same difference observed in $M(T)$ of Fig. 1(a) at 270 K. The increase of B_{hf} implies a reinforcement of the local magnetic field related with the annealing of defects and the recovery of the FM coupling.

With respect to the MT, it is noteworthy that the recovery of the atomic scale magnetism and the annihilation of dislocations and defects does not affect the equilibrium temperature between the austenitic and martensitic phase, T_0. As shown in Fig. 4, T_0 remains constant irrespectively of the annealing temperature. T_0 is highly sensitive to the atomic order[58] and its constant value reiterates the lack of differences in atomic disorder throughout the studied samples. However, the temperature range in which the MT is extended (M_s-M_f) decreases from 92.5 K down to 70 K between the Milled and AN873 sample (see Fig. 4).

As the annealing temperature increases, the non-magnetic regions close to the dislocations decrease and the intensity of the non-magnetic component revealed by MS decreases as well. The MS singlet is then directly related to the internal stress-state and the distorted regions that ultimately affects the MT. Therefore, the influence of the microstructural recovery on the MT can be directly tracked by the singlet component revealed by ^{119}Sn MS. In this respect, the inset in Fig. 4 shows the direct relationship between the intensity of the MS singlet and the width of the temperature range of the MT. As soon as the non-magnetic regions decrease due to the annealing, the M_s-M_f does behave in the same way.

In conclusion, we show that both MT and magnetic properties of $Ni_{50}Mn_{35}Sn_{15}$ are very sensitive to slight microstructural distortions even without inducing any change in atomic disorder. Due to the high stability that Ni-Mn-Sn systems show against the atomic disorder, this result opens an additional way to properly tune the functional properties in these systems. Finally, we show that ^{119}Sn MS can be used to link the MT with the microstructural state, becoming a practical tool to assess the microstructural characterization of the local stress and defect state in order to properly tune the MT towards future applications.

This work is supported for the Basque Government Grant IT-1005-16 by the Spanish Ministry of Economy and Competitiveness under the project MAT2015-65165-C2-R (MINECO/FEDER) and GIC1585. I. Unzueta also wants to acknowledge the Basque Government Grant PRE-2014-214. ILL and SpINS are acknowledged for beam time allocation. J. López-García acknowledges ILL for his PhD. contract.

REFERENCES

[1] K. Ullakko, J. K. Huang, C. Kantner, R. C. O'Handley, and V. V. Kokorin, Appl. Phys. Lett. **69**, 1966 (1996).

[2] M. Chmielus, X. X. Zhang, C. Witherspoon, D. C. Dunand, and P. Mullner, Nat. Mater. **8**, 863 (2009).

[3] S. Y. Yu, Z. H. Liu, G. D. Liu, J. L. Chen, Z. X. Cao, G. H. Wu, B. Zhang, and X. X. Zhang, Appl. Phys. Lett. **89**, 162503 (2006).

[4] W. Ito, K. Ito, R. Y. Umetsu, R. Kainuma, K. Koyama, K. Watanabe, A. Fujita, K. Oikawa, K. Ishida, and T. Kanomata, Appl. Phys. Lett. **92**, 021908 (2008).

[5] A. Planes, L. Mañosa, and M. Acet, J. Phys. Condens. Matter **21**, 233201 (2009).

[6] L. Mañosa, D. González-Alonso, A. Planes, E. Bonnot, M. Barrio, J.-L. Tamarit, S. Aksoy, and M. Acet, Nat. Mater. **9**, 478 (2010).

[7] Z. D. Han, D. H. Wang, C. L. Zhang, H. C. Xuan, B. X. Gu, and Y. W. Du, Appl. Phys. Lett. **90**, 042507 (2007).

[8] T. Krenke, E. Duman, M. Acet, E. F. Wassermann, X. Moya, L. Manosa, and A. Planes, Nat. Mater. **4**, 450 (2005).

[9] M. Khan, I. Dubenko, S. Stadler, and N. Ali, Appl. Phys. Lett. **91**, 072510 (2007).

[10] Y. B. Yang, X. B. Ma, X. G. Chen, J. Z. Wei, R. Wu, J. Z. Han, H. L. Du, C. S. Wang, S. Q. Liu, Y. C. Yang, Y. Zhang, and J. B. Yang, J. Appl. Phys. **111**, 07A916 (2012).

[11] Y. Sutou, Y. Imano, N. Koeda, T. Omori, R. Kainuma, K. Ishida, and K. Oikawa, Appl. Phys. Lett. **85**, 4358 (2004).

[12] K. Oikawa, W. Ito, Y. Imano, Y. Sutou, R. Kainuma, K. Ishida, S. Okamoto, O. Kitakami, and T. Kanomata, Appl. Phys. Lett. **88**, 122507 (2006).

[13] R. Kainuma, Y. Imano, W. Ito, Y. Sutou, H. Morito, S. Okamoto, O. Kitakami, K. Oikawa, A. Fujita, T. Kanomata, and K. Ishida, Nature **439**, 957 (2006).

[14] R. Kainuma, Y. Imano, W. Ito, H. Morito, Y. Sutou, K. Oikawa, A. Fujita, K. Ishida, S. Okamoto, O. Kitakami, and T. Kanomata, Appl. Phys. Lett. **88**, 192513 (2006).

[15] T. Krenke, M. Acet, E. F. Wassermann, X. Moya, L. Mañosa, and A. Planes, Phys. Rev. B **73**, 174413 (2006).

[16] X. Moya, L. Mañosa, A. Planes, S. Aksoy, M. Acet, E. F. Wassermann, and T. Krenke, Phys. Rev. B **75**, 184412 (2007).

[17] Z. D. Han, D. H. Wang, C. L. Zhang, S. L. Tang, B. X. Gu, and Y. W. Du, Appl. Phys. Lett. **89**, 182507 (2006).

[18] P. A. Bhobe, K. R. Priolkar, and A. K. Nigam, Appl. Phys. Lett. **91**, 242503 (2007).

[19] J. L. S. Llamazares, H. Flores-Zúñiga, D. Ríos-Jara, C. F. Sánchez-Valdes, T. García-Fernández, C. A. Ross, and C. García, J. Appl. Phys. **113**, 17A948 (2013).

[20] M. Acet, Nat. Mater. **8**, 854 (2009).

[21] R. Niemann, O. Heczko, L. Schultz, and S. Fähler, Appl. Phys. Lett. **97**, 222507 (2010).

[22] J. Feuchtwanger, M. L. Richard, Y. J. Tang, A. E. Berkowitz, R. C. O'Handley, and S. M. Allen, J. Appl. Phys. **97**, 10M319 (2005).

[23] J. Liu, N. Scheerbaum, S. Kauffmann-Weiss, and O. Gutfleisch, Adv. Eng. Mater. **14**, 653 (2012).

[24] M. Schmitt, A. Backen, S. Fähler, and M. Kohl, Microelectronic Engineering **98**, 536 (2012).

[25] M. Kohl, D. Brugger, M. Ohtsuka, and T. Takagi, Sens. Actuator A-Phys. **114**, 445 (2004), selected papers from Transducers 03.

[26] C. Biffi and A. Tuissi, Opt. Laser. Technol. **78, Part B**, 42 (2016).

[27] S. V. Kumar, R. Singh, M. M. Raja, A. Kumar, S. Bysakh, and M. Mahendran, Intermetallics **71**, 57 (2016).

[28] K. V. Peruman, S. Vinodh Kumar, K. Pushpanathan, and M. Mahendran, Funct. Mater. Lett. **04**, 415 (2011).

[29] J. Ortín and A. Planes, Acta Metall. **36**, 1873 (1988).

[30] A. Roytburd, T. Kim, Q. Su, J. Slutsker, and M. Wuttig, Acta Mater. **46**, 5095 (1998).

[31] V. Sánchez-Alarcos, V. Recarte, J. Pérez-Landazábal, S. Larumbe, R. Caballero-Flores, I. Unzueta, J. García, F. Plazaola, and J. Rodríguez-Velamazán, J. Alloy. Comp. **689**, 983 (2016).

[32] A. A. Prasanna and S. Ram, Sci. Tech. Adv. Mater. **14**, 015004 (2013).

[33] H. Scherngell and A. Kneissl, Acta Mater. **50**, 327 (2002).

[34] G. Rao, J. Wang, E. Han, and W. Ke, Mater. Lett. **60**, 779 (2006).

[35] A. Ghotbi Varzaneh, P. Kameli, V. R. Zahedi, F. Karimzadeh, and H. Salamati, Met. Mater. Int **21**, 758 (2015).

[36] A. L. Alves, E. C. Passamani, V. P. Nascimento, A. Y. Takeuchi, and C. Larica, J. Phys. D: Appl. Phys. **43**, 345001 (2010).

[37] G. D. Liu, X. F. Dai, H. Z. Luo, H. Y. Liu, F. B. Meng, Y. Li, X. Yu, J. L. Chen, and G. H. Wu, J. Phys. D: Appl. Phys. **44**, 045002 (2011).

[38] A. Ghosh and K. Mandal, Appl. Phys. Lett. **104**, 031905 (2014).

[39] V. Sànchez-Alarcos, J. Pèrez-Landazàbal, V. Recarte, I. Lucia, J. Vèlez, and J. Rodrìguez-Velamazàn, Acta Mater. **61**, 4676 (2013).

[40] E. C. Passamani, C. Córdova, A. L. Alves, P. S. Moscon, C. Larica, A. Y. Takeuchi, and A. Biondo, J. Phys. D: Appl. Phys. **42**, 215006 (2009).

[41] R. Y. Umetsu, R. Kainuma, Y. Amako, Y. Taniguchi, T. Kanomata, K. Fukushima, A. Fujita, K. Oikawa, and K. Ishida, Appl. Phys. Lett. **93**, 042509 (2008).

[42] R. Y. Umetsu, K. Sano, K. Fukushima, T. Kanomata, Y. Taniguchi, Y. Amako, and R. Kainuma, Metals **3**, 225 (2013).

[43] E. Passamani, V. Nascimento, C. Larica, A. Takeuchi, A. Alves, J. Proveti, M. Pereira, and J. Fabris, J. Alloy. Comp. **509**, 7826 (2011).

[44] J. López-García, J. I. Pérez-Landazábal, V. Recarte, J. A. Rodríguez-Velamazán, V. Sánchez-Alarcos, and I. Unzueta, 10.5291/ILL-DATA.5-24-591 (2016).

[45] J. Rodríguez-Carvajal, Physica B **192**, 55 (1993) The programs of the FullProf Suite can be obtained at http://www.ill.eu/sites/fullprof/.

[46] V. V. Sokolovskiy, V. D. Buchelnikov, M. A. Zagrebin, P. Entel, S. Sahoo, and M. Ogura, Phys. Rev. B **86**, 134418 (2012).

[47] T. Krenke, M. Acet, E. F. Wassermann, X. Moya, L. Mañosa, and A. Planes, Phys. Rev. B **72**, 014412 (2005).

[48] O. C. Kistner and A. W. Sunyar, Phys. Rev. Lett. **4**, 412 (1960).

[49] F. J. B. Dominic P. E. Dickson, *Mössbauer Spectroscopy* (Cambridge University press, Berlin, 1986).

[50] J. Schaf, K. L. Dang, P. Veillet, and I. A. Campbell, J. Phys. F: Metal Physics **13**, 1311 (1983).

[51] H. Y. H. W. H. S. Takeshi Shinohara, Katuji Sasaki and T. Okada, J. Phys. Soc. Jpn. **50**, 2904 (1981).

[52] K. Ikeda and S. Takahashi, Phys. Rev. B **30**, 3808 (1984).

[53] S. Takahashi and T. Shinohara, J. Phys. F: Metal Physics **12**, 3115 (1982).

[54] A. P. Young and J. P. Jakubovics, J. Phys. F: Metal Physics **5**, 1866 (1975).

[55] T. Kamiyama, T. Shinohara, S. Tomiyoshi, Y. Minonishi, H. Yamamoto, H. Asano, and N. Watanabe, J. Appl. Phys. **68**, 4741 (1990).

[56] D. Merida, J. A. García, V. Sánchez-Alarcos, J. I. Pérez-Landazábal, V. Recarte, and F. Plazaola, Appl. Phys. Lett. **104**, 231905 (2014).

[57] P. K. Michael Kalvius, *The Rudolf Mössbauer Story* (Springer-Verlag Berlin Heidelberg, 2012).

[58] V. Sánchez-Alarcos, V. Recarte, J. Pérez-Landazábal, C. Gómez-Polo, and J. Rodríguez-Velamazán, Acta Mater. **60**, 459 (2012).